Conference Title: CSNI Specialist Meeting on International Depressurization

Date & Place: June 15, 1989 -- Garching, Germany

# INVESTIGATION OF REACTOR COOLANT SYSTEM DEPRESSURIZATION AS AN ACCIDENT MANAGEMENT STRATEGY

D. W. Golden
Idaho National Engineering Laboratory
EG&G Idaho, Inc.
Idaho Falls, Idaho (United States)

F. Odar
United States Nuclear Regulatory Commission
Rockville, Maryland (United States)

J. D. Miller
Idaho National Engineering Laboratory
EG&G Idaho, Inc.
Falls, Idaho (United States)

## ABSTRACT

An investigation of intentional depressurization of the reactor coolant system (RCS) as a means to mitigate direct containment heating (DCH) is presented in this paper. Primary and secondary feed-and-bleed strategies are considered as basic options to prevent core damage. For a station blackout, where the ac power is lost, there is no safety injection. For a TMLB' transient, the additional failure of the auxiliary feedwater is assumed. For this transient, a primary or secondary feed-and-bleed strategy using existing systems is not possible because of unavailability of the safety injection and auxiliary feedwater. The operators can take action to depressurize the primary system using the pressurizer power-operated relief valves (PORV), take no action, or find an emergency source of water independent of ac power to perform a feed-and-bleed operation. The last option may require some minor plant system modifications.

Analyses for depressurization of the Surry Nuclear Power Plant are being performed using the SCDAP/RELAP5 code for a hypothetical TMLB' sequence. Two cases with different times for the initiation of depressurization are considered. In the first case, the depressurization is initiated at the time of steam generator dry out. This case is called early depressurization. In the second case, the depressurization is initiated at the time of core uncovery. This case is called late depressurization. Both calculations show that the system can be depressurized to the level that DCH may be minimized. In the early depressurization, the surge line may also fail, leading to rapid depressurization of the primary. In the late depressurization, surge line failure is not predicted.

Uncertainties in these calculations are discussed, and different strategies are evaluated based on engineering judgment. These strategies, in the order of preference, are: (a) perform feed-and-bleed operation if the ac power is recovered within a certain period of time; (b) establish an emergency source of feedwater independent of the ac power for a feed-and-bleed operation; (c) depressurize the primary system if an emergency source of feedwater is not available; and (d) take no action.

## I. Introduction

Intentional depressurization of the reactor coolant system (RCS) is being investigated as a potential means of mitigating direct containment heating (DCH). A DCH event could occur as the result of the dispersal of molten core materials into the containment caused by a high-pressure core melt ejection [1]. The probability of occurrence for a DCH event is primarily a function of the driving pressure for the core melt ejection, the quantity of the molten core ejected, and the composition of the core melt. By reducing the driving pressure the degree of direct containment heating, and thus the challenge to containment is reduced. A possible functional relationship is depicted *conceptually* in Figure 1. The boundaries between the occurrence and nonoccurrence of DCH are the lines separating regions A and B from region C. In regions A and B, either the RCS pressure will provide an insufficient driving force to disperse the molten corium in the containment or there will be insufficient energy content within the melt to cause DCH. It should be kept in mind that these boundaries are not well established and may not even be distinct.

The purpose of the analyses presented in this paper is to evaluate the ability to mitigate the potential for DCH during a severe core damage accident by intentional depressurization of the RCS. That is, to evaluate the capability to reduce RCS pressure to a level that minimizes the potential for DCH (places plant conditions in region A of Figure 1) at the time of reactor pressure vessel (RPV) breach. The plant operators have indications of RCS pressure, but there is little if any plant instrumentation that will indicate the quantity, composition, and location of molten corium during a severe accident. The required steps in the evaluation process are to (a) identify potential depressurization strategies, (b) evaluate the effectiveness of each strategy, (c) identify and evaluate the potential negative effects of each strateg. nd (d) determine the net benefit associated with each strategy.

Potential strategies for prevention of DCH are (a) perform a feed-and-bleed operation if ac power is recovered within a certain period of time, (b) establish an emergency source of feedwater independent of the ac power for a feed-and-bleed operation, (c) depressurize the system if an emergency source of feedwater is not available, and (d) take no action. There has been extensive research conducted by the U. S. Nuclear Regulatory Commission (NRC) regarding the first strategy. Loomis and Cozzuol [2] reviewed the research on primary system feed-and-bleed and concluded that this strategy is a viable technique to maintain control of primary system pressure and temperature. Successful feed-and-bleed requires that the energy flow out of the system be equal to or greater than decay heat and that the mass flow out of the system be replaced by the safety injection system or charging pumps. The Severe Accident Sequence Analysis (SASA) Program analyzed nuclear plant transients likely to lead to a severe accident. For a station blackout, all ac power except that derived from battery-driven inverters is lost. In the station blackout transient sequence, safety injection is not available and feed-and-bleed cannot be established. Analyses of station blackout sequences performed at the Idaho National Engineering Laboratory [3] under SASA's sponsorship provide a basis to conclude that if auxiliary feedwater

is available or is recovered from about 10 to 28 minutes (a function of the plant analyzed) prior to core uncovery, or if ac power is restored 14 to 38 minutes prior to core uncovery (interpreted as no core damage), core damage can be prevented.[1] Thus, either a primary or secondary feed-and-bleed operation is expected to prevent core damage if flows are established within a certain time.

For a TMLB' sequence, the loss of auxiliary feedwater is assumed in addition to a station blackout. Thus, neither primary nor secondary feed-and-bleed are available. Depressurization of the RCS requires one of the three remaining strategies to accomplish depressurization. Analyses performed using the SCDAP/RELAP5 integrated severe accident analysis code to evaluate these strategies are the subject of this paper. The following sections provide a review of the relevant assessment data base and analytical methodology (Section II) results of the analyses (Section III), a discussion of operational uncertainties (Section IV), and conclusions (Section V).

## II. Assessment Data Base and Analytical Methodology

Extensive research sponsored by the NRC and others on feed-and-bleed has shown this strategy to be a viable technique to prevent core uncovery when electric power is available. The research results also provide a data base to assess the adequacy of code models that are intended to predict plant thermal-hydraulics during feed-and-bleed. Experiments conducted in the Loss of Fluid Test Facility (LOFT), Semiscale, MIST, OTIS, and ROSA-IV form the assessment data base for analytical tools such as RELAP5 [4,5] and TRAC [6]. Loomis and Cozzoul's [2] review of feed-and-bleed included a review of code comparisons for both RELAP5 and TRAC to the experimental data. They concluded that the codes predicted the phenomenology of feed-and-bleed, but did not match event timing as well.

The analyses presented in this paper consider depressurization by opening the PORVs. It is expected that the flow through the PORVs will be choked (limited to sonic or critical velocity) until the RCS pressure is nearly equal to the containment pressure. Therefore, the performance of the critical flow model in SCDAP/RELAP5 is of particular importance. The SCDAP/RELAP5 critical flow model calculates the velocity of sound in a two-phase, two component mixture based on the equation of state [7]. The critical flow model at low quality has been identified by the International Code Assessment Program (ICAP) [8] as one of the three main code deficiencies. The discrepancy was found to be most notable for a small break with low-quality, saturated flow that occurred over an extended period of time. The PORVs are at the top of the pressurizer. At the time the PORVS are assumed to be latched open, it is expected that the pressurizer will rapidly drain or will have already drained. A saturated, low-quality flow will exist at the PORVs for at most a brief

---

1. In both cases described, the analyses are plant-specific. While a broad interpretation about feed-and-bleed may be generally appropriate, there may be specific plants that could require much earlier initiation of feed-and-bleed or unusual procedures to initiate feed-and-bleed. Also, Combustion Engineering's System 80 plants, which do not have power-operated relief valves (PORVs), are incapable of feed-and-bleed or direct primary system depressurization.

time. Therefore, the uncertainties associated with the critical flow model will not have a significant effect on the results.

A datum for sequences leading to late-phase core melt progression (formation of a molten pool in the core region and relocation of molten material to the lower plenum) is represented by the TMI-2 accident. A detailed description of the TMI-2 accident and the research findings of the TMI-2 Accident Evaluation Program are provided in "A Scenario of the TMI-2 Accident" [9]. The TMI-2 accident was a small break loss of coolant accident (LOCA) through the stuck-open PORV without adequate safety injection. (The operators bypassed safety injection early in the accident.) Eventually, the core uncovered and approximately 50% of the core melted. About 20 tonnes of the molten material flowed to the lower plenum. The RPV did not fail, and the molten material in the reactor vessel was cooled after safety injection was established by the operators. Since the accident embodies many of the possible events in a severe accident and is a unique datum for light water reactors, the TMI-2 Analysis Exercise is being conducted through the sponsorship of the Committee on the Safety of Nuclear Installations (CSNI) to benchmark severe accident analysis codes [10]. Users and developers of many of the severe accident analysis codes, including SCDAP/RELAP5 [11] and MELPROG/TRAC [12], are participating in the analysis exercise.

Up to the time of initial core melting, most of the codes match the recorded plant data, such as RCS pressure, reasonably well. Preliminary results from the various codes have a relatively wide spread beyond initial core melting, while generally following the trend of the recorded RCS pressure. This was particularly evident in the calculations of total hydrogen generation. The calculated total hydrogen at 174 minutes (the end time of the first two phases of the analysis exercise) varied from about 100 to 460 kg. This compares to an estimated release of about 300 kg [13, 14] at 174 minutes. Similar variances occurred for other calculated quantities. It is noted that some of the boundary conditions, particularly the high-pressure injection rate, may have large uncertainties due to the lack of recorded flow measurements. Since an effort has been made to compare the codes based on a common set of boundary conditions, the variations noted are apparently real. Therefore, it is concluded that there are potentially large uncertainties in the core damage progression models that need to be accounted for in an analysis of intentional depressurization.

The analytical approach used to model late-phase core melt progression herein has been to bound the uncertainties in the core melt progression parameters that are believed to affect RCS pressure [15]. The methodology shown in Figure 2 relies on performing calculations to target core damage states. The parametric analysis is started from the first target state, which is core heatup. The second target state is the formation of a molten pool within the core region. The third state is failure of the lower head caused by interactions with relocated molten core materials.

It is expected that any calculation that extends from core heatup will eventually calculate the formation of a molten pool. The parameters that control the calculated core damage progression were varied over their range of expected values to minimize and maximize RCS pressure. On path 1 (the upper line from core heatup to molten pool formation), the intent is to maximize steam interactions and oxidation of the cladding. This was accomplished first by holding molten metallic cladding in place as long as possible via SCDAP/RELAP5 input parameters affecting the cladding oxide

shell failure. The failure temperature of the oxide shell, which holds molten metallic cladding in place, was set to its upper bound, and the minimum oxide shell thickness required to hold molten metallic cladding in place was set to its lower bound. This increases the total cladding oxidation and hence the energy generated by oxidation. The second set of parameters required to maximize RCS pressure control the formation of rubble debris beds composed of fractured, embrittled fuel rods. Fracture of oxidized cladding from cooling is caused by the injection of accumulator water when the RCS is depressurized to below the accumulator tank pressure. Once the cladding has been oxidized to a maximum beta Zr thickness of 0.0001 m [16], the cladding will become embrittled upon cooling to a specified temperature. The embrittlement temperature was varied from a maximum value of 1273 K to a minimum value of Tsat + 90 K. The maximum value assumes the energy associated with the $ZrO_2$ phase change at 1273 K is sufficient to shatter oxidized cladding. The minimum value is based on shattering the cladding at a specified temperature above the saturation temperature. The fragmented cladding has a larger surface-to-volume ratio, hence the heat transfer rate from the debris to the steam coolant should be greater and the calculated RCS pressure will be greater than for an intact rod geometry. The parameters for path 2 (bottom line from core heatup to molten pool formation) maximize relocation of molten metallic cladding, and minimize rubble debris formation. This is the opposite of path 1. The variations used in the analyses are summarized in Table I.

It is expected that once the molten pool is formed it will eventually melt through any supporting crust and at least some of the molten core materials will relocate to the RPV lower head. Heat transfer from the debris bed formed by this process will heat up the lower head and could cause it to fail by either creep rupture or melting. If the calculation models a maximum heat transfer to the coolant in the lower plenum, the pressure will be maximized. Further, this will remove some energy from the debris bed that could be transferred to the lower head. Thus, the calculated time to RPV failure will be increased compared to a calculation that minimizes the heat transfer to the coolant. Path 3 (top line from molten pool to RPV failure) is based on maximizing the heat transfer from debris to coolant. Path 4 (bottom line from molten pool to RPV failure) minimizes the heat transfer from debris to coolant.

The SCDAP/RELAP5 model for relocation transfers relocating molten material to the lower head over a user-specified time. (A time of 100 s was used in these calculations based on estimates for the TMI-2 relocation.) At each time step, heat transfer from the calculated quantity of relocating material to the coolant is determined. Heat transfer to the coolant is maximized[2] if during each time step the relocating material is cooled to the saturation temperature (quenched). The code model for path 3 uses this algorithm unless the energy removed during any time step would require more liquid to be evaporated than exists in the RELAP5 lower head volume. For path 4, no energy is transferred from the relocating debris. Once the debris bed forms on the lower head, heat transfer to the coolant is controlled by the

---

2. The current code version considers heat transfer only to the coolant in the lower plenum volume. Thus, heat transfer to any coolant present in the core region will not be included in the calculation. For this analysis, the only coolant present at relocation is the coolant in the lower plenum and the core entrance volumes, and the model limitation is of no real importance.

porosity of the debris bed, with high porosity producing a greater energy exchange.

Once the material is in the lower head volume, the heat transfer from the debris bed to the coolant and lower head is calculated by a two-dimensional, finite-element model. The porosity of the debris bed was set to 0.5 to maximize heat transfer to the coolant and RCS pressure (path 3). For path 4, the porosity was set to approximately 0 to minimize heat transfer to the coolant and RCS pressure.

Analyses for three depressurization strategies have been completed or are in the process of being completed. The first is an analysis of the no-action strategy. The second strategy is to depressurize by latching open the PORVs at steam generator dry out. This is called early depressurization. For the early depressurization strategy, the analysis cases shown in Table I were performed. The third strategy analyzed is to depressurize by latching open the PORVs when the core uncovers. This is called late depressurization. Core uncovery was defined to be when the maximum core exit fluid temperatures reached ~922 K (1200 °F). The late depressurization analysis for path 1 is currently being performed and is at the point of initial in-core cladding relocation. The results of analyses for these three strategies are presented in Section III.

## III. SCDAP/RELAP5 Analysis of a Surry Station Blackout.

Surry is a two-unit nuclear power station. The units are Westinghouse 3-loop nuclear steam supply systems with U-tube steam generators. Surry was chosen for these analyses since it is one of the reference plants for NUREG-1150 [1]. The three depressurization strategies considered in this analysis to mitigate DCH in Surry are to (a) open the PORVs early at steam generator dryout; (b) open the PORVs late at the start of core heatup; or (c) no operator action. The analysis by Bayless [17] to study hot leg counter current and in-vessel natural circulation provides an analysis of the no-operator action strategy. Bayless performed sensitivity studies over a wide range of parameters that control energy transport within the RCS. The results of the sensitivity studies predict failure of the pressurizer surge line between about 230 and 260 min for a TMLB'. If the pressurizer surge line were to fail during a station blackout sequence, then the RCS would be rapidly depressurized to containment pressure and DCH would then be mitigated. Yet, the prediction of surge line failure remains highly uncertain due to the uncertainties in core damage progression and the dependence on hot leg counter current natural circulation to transport the energy to the surge line entrance.

Chambers [15,18] performed the calculations listed in Table I for the early depressurization strategy up to the time of molten pool relocation to the lower plenum. Various events occurring for Paths 1 and 2 are summarized in Table II. Except for the timing of initial cladding relocation, there is little difference between the two calculations. The calculated pressurizer level is shown in Figure 3. The pressurizer drains rapidly and is empty by 180 minutes. The period of time that low quality, saturated flow is calculated to exist at the PORVs is short relative to the total transient time. Therefore, any discrepancy in the critical flow model for low- quality, saturated flow, as mentioned in Section II, is relatively insignificant. The calculated RCS pressures for paths 1 and 2 (calculations 6 and 7) are shown in Figure 4. The two

main features of this plot are the cyclic behavior of the calculated RCS pressure and the small difference between the two calculations. The cause of both features is the phenomenology of the accumulator injection process. When RCS pressure first reaches the accumulator pressure, liquid is injected into the primary and it enters the core region. This increases the vapor generation rate. The increased vapor generation rate is greater than the volumetric outflow through the PORVs. Thus, RCS pressure increases and shuts off the accumulator flow. Eventually, the vapor generation rate decreases and the PORVs are again able to reduce RCS pressure. The cycles repeat until the accumulators are empty. The thermal-hydraulics models exercised by the accumulator injection process appear to control the calculated system response. Thus, the uncertainties considered in the parameter variations are calculated to have little effect on the calculated RCS pressure. Subjectively, this implies that for depressurization the details of the thermal-hydraulics of the accumulator injection process are more important than the uncertainties in core melt progression up to the time the accumulators empty.

As shown in Figure 4, the pressure oscillations initially are quite small. The small pressure oscillations indicate that the flow from the accumulators is correspondingly small. This effect can also be seen in core temperatures. The calculated cladding temperatures at the top of the core, as shown in Figure 5, rapidly escalate to in excess of 2000 K. Eventually, the accumulator flow is sufficient to turn around the temperatures, but only temporarily. By 250 min the upper region of the core is calculated to reheat.

Figure 6 shows a map of the calculated domain of the molten pool at the time of relocation to the lower plenum for paths 1 and 2. Path 1 (calculation 6) with the maximum fragmentation and minimum relocation is calculated to produce the larger molten pool. On the other hand, the minimum fragmentation and maximum relocation case (calculation 7) results in more fuel and cladding to be relocated downward in the core. With more material lower in the core, there is more material at lower temperatures; therefore, a smaller molten pool is calculated for the maximum relocation case. Uncertainties in the core melt progression models are thus concluded to be important to the calculation of total core melt and the geometry of the damaged core.

The path 1 calculation was continued on path 3 to about 550 min. (9.2 h). Approximately 70 tonnes of core material were calculated to flow from the molten pool through the failed lower crust. The flow was assumed to occur over a period of 100 s. The molten core materials were assumed to transfer sufficient energy to the lower plenum coolant to reduce the temperature of the relocating debris to the saturation temperature. Once the vapor void fraction in the RELAP5 lower head volume was calculated to be approximately one, the energy transfer was terminated. This resulted in a calculated pressure increase of about 2 MPa, as shown in Figure 7. The only significant heat transfer was then calculated to be to the lower head. The calculations predict the debris bed to initially cool as energy is transferred to the lower head. Once the lower head starts to heat up, the heat transfer rate decreases and ultimately the debris bed reheats. The calculations were terminated when it was noticed that the code was not predicting creep of the lower head due to the fact that RCS pressure was calculated to be nearly equal to containment pressure. It was found that the flow-through the PORVs was not choked for significant time periods even during much of the accumulator injection. The containment, having been modeled as

a single volume without heat structures, allowed the calculated containment pressure to increase to an unrealistically high value. If the calculation had been continued without modifications, it is expected that the code would have predicted lower head meltthrough at about 600 min. If the containment volume and heat structures were modeled, it is expected that the code would have predicted a pressure below 1 MPa (145 psia). Since this calculation generally provided the needed information, it was decided to run the late depressurization calculation with an improved containment model. The late depressurization case was calculated in parallel with a 15 volume MELCOR [19] containment model with heat structures using the PORV flows calculated by SCDAP/RELAP5. The MELCOR containment pressure was fed back to the SCDAP/RELAP5 calculations as needed and the two codes were thus used in an iterative manner.

An additional feature of the early depressurization calculation was the prediction of surge line failure at 166 (path 1) and 172 (path 2) min. If uncertainties in calculation were small, then we could be certain that DCH would be mitigated by rapid depressurization caused by the surge line failure. The pressure time history for this case is shown in Figure 8. Surge line failure in this calculation is significantly less uncertain then the no-action case, since the analysis does not depend on natural circulation to bring hot gasses to the surge line entrance. However, the analysis does depend on the core heatup sequence and core damage progression to provide the hot gasses with the correct timing for surge line failure to be predicted. Thus, the prediction of surge line failure as a means of RCS depressurization and mitigation of DCH depends on uncertainties in core melt progression.

The late depressurization strategy assumes that the operators open the PORVs at core uncovery as defined by the core exit thermocouples reading ~922 K (1200 °F). For the late depressurization calculation, paths 1 and 3 are being followed with the same parameter settings as in the early depressurization calculation (calculation 6). The calculated pressure for the three strategies is shown in Figure 8. Since the late depressurization starts after some superheating exists in the RCS, there is no subcooled blowdown as evidenced in the early depressurization case. The late depressurization case predicts fewer accumulator cycles,with greater flow in each cycle. As such, the late depressurization calculation shows the accumulators emptying slightly ahead of the early depressurization case. This behavior is a direct result of the lower containment pressure. When the accumulators had emptied in the late depressurization calculation, MELCOR had calculated the containment pressure to be about 0.2 MPa (~30 psia).

The character of the calculated system response is quite different for late depressurization. First, it is noted that the accumulators empty at about the same time for both early and late depressurization. This suggests that the average accumulator inflow rate is greater for late depressurization. This difference in calculated response is significant to the calculation of core heatup and core damage progression. Comparisons of accumulator flows and total hydrogen generated are shown in Figures 9 and 10. The initial response for early depressurization (Figure 9) indicates that the vapor generation rate in the core region is sufficient to maintain system pressure at a level that allows only a slow influx from the accumulators for about the first hour of accumulator injection. This is calculated to be insufficient to cool the upper regions of the core. Core heatup continues, and about 220 kg of hydrogen are generated. The initial response for late depressurization (Figure 10) indicates that condensation is

sufficient to lower the pressure sufficiently to allow a large influx of accumulator water. This is followed by a rapid increase in vapor generation as the mixture level in the core increases. Cooling is provided over the entire core volume. Therefore, the hydrogen generation was calculated to cease on the first injection cycle. Core heatup did not restart until the accumulators were emptied. This behavior is probably due to the difference in RCS void fraction at the time of PORV opening. The greater void fraction for late depressurization appears to enhance condensation and the effect of condensation on RCS pressure.The predicted total hydrogen generation for the early and late depressurizations is quite different. The hydrogen generation rates for the two cases are also shown in Figures 9 and 10. The calculated cooling is more effective for the late depressurization case, and core heatup and hydrogen generation are delayed compared to the early depressurization case. This is also shown in Figure 11 by the calculated cladding temperature at the top of the core. The accumulator inflow is able to maintain calculated temperatures below runaway oxidation. Because of the lower temperatures, surge line failure has not yet been calculated to occur. Extrapolation of the surge line heatup rate suggests that the high-temperature transient will end prior to the surge line reaching the melting point. Thus, the surge line may not fail in the late depressurization case. This hypothesis will be confirmed or rejected by continuation of the calculations.

A comparison of event timing for the three strategies is shown in Table III. Subjectively, late depressurization provides the most time for the operators to recover ac power and/or auxiliary feedwater. Therefore, late depressurization may be preferred over early depressurization. If the operators take no action to depressurize, then failure of the surge line is predicted, and this would depressurize the RCS.

It is noted that there were some difficulties with the code in accomplishing the late depressurization calculation. The code on two occasions failed due to water property errors that were not alleviated by reducing the maximum time step. This is usually an indication that the energy transfer at the interface between SCDAP and RELAP5 are inconsistent. While the offending code model was being sought out, the calculation was patched. Since the core was in general being cooled even at its top (see Figure 11) by the accumulator flow, the PORVs were closed just prior to the water property error and held closed to allow the code to reheat the core slightly and stabilize the calculation. This is conservative with regard to the calculation of RCS pressure. The periods of closed PORVs are clearly indicated by (Figure 8) the repressurizations at about 250 min and 290 min.[3]

An independent calculation of the station blackout sequence for Surry was performed [20] using MELPROG/TRAC. The calculation was different from a TMLB` sequence because a pump seal LOCA was also modeled (TMLB`-S3). Preliminary evaluations indicate there are similarities and significant differences between the SCDAP/RELAP5 and MELPROG/TRAC calculations. The main differences relate to the predicted behavior during accumulator injection and

---

3. The interface model for rubble debris heat transfer in the situation where the temperature is decreasing was found to be inappropriate for a high-void-fraction environment. This resulted in the excess extraction of energy from the liquid phase on the RELAP5 side of the code.

relocation of molten material to the lower plenum. Detailed comparisons of the two code calculations are planned to help determine the causes for the different results. A SCDAP/RELAP5 calculation of the TMLB'-S3 sequence is being performed by the Japan Atomic Energy Research Institute, which will provide a more direct comparison of the two codes.

The major uncertainties in both sets of analyses relate to event timing, degree of core melt, quantity of hydrogen generated, and RCS pressure. The cited uncertainties are important to the evaluation of potential negative aspects of depressurization. These include the potential for early release of hydrogen to the containment, along with increased hydrogen generation. There is still a debate regarding the increased potential for molten fuel-coolant interactions at low pressures. This could cause a very large increase in pressure at the time of molten pool relocation to the lower plenum. Further study of the potential negative effects may show depressurization to be a less desirable strategy than a no-action strategy.

One remaining strategy is to obtain an emergency source of auxiliary feedwater from a non-traditional source. For Surry, the firewater system is connected to the suction of the auxiliary feedwater pumps. A diesel-driven fire pump [21] capable of pumping 2500 gallons per minute at a rated discharge head of 100 psi is available at the plant site. This pump takes suction from one of two tanks, each containing 250,000 gallons of water. Opening a line to provide water to the suction of the auxiliary feedwater pumps requires the opening of three valves. If the valves can be properly aligned and pressure in the steam generator can be reduced to a level that the pump head is sufficient to provide flow to the steam generators, it would be possible to prevent core heatup for an extended period of time. This is essentially a secondary feed (via the fire pump) and bleed (via blowdown into the main condenser and condenser venting) operation.

**IV. Operational uncertainties.**

There are two types of operational uncertainties in the depressurization strategies. First, will the operators be able to accomplish the tasks required to depressurize the plant? Second, will the equipment be available, and will it function without failure?

An assessment of the capability of the operators at Surry to successfully initiate depressurization was performed. The assessment included an evaluation of the existing Emergency Operating Procedures (EOPs), a disclosure of the factors that effect decision making for the scenario considered, and a human reliability analysis (HRA) for the critical actions necessary to accomplish depressurization. The results of the assessment indicate that implementing depressurization is dependent upon training and procedural guidance (preparedness) and the time available to make decisions and take appropriate actions. It was also disclosed that, because of the EOP structure, depressurizing the RCS to avoid DCH conditions would be a decision made outside the guidance provided by the EOPs.

Because of the difficulty in establishing the amount of time available to the operator to perform the critical recovery actions, a broad range of uncertainty accompanied the probability of the operator to successfully initiate depressurization. Through sensitivity analyses, it was determined that the factor which dominates the

probability to perform RCS depressurization is the time available to diagnose the need to depressurize [22]. This is due to concurrent, ongoing activities to recover both ac power and a mechanism to provide feedwater to a steam generator. It is also due to the sharp temperature rise (and a rapidly shrinking time window to perform mitigative actions) when core exit thermocouples reach superheated conditions.

If the PORVs fail closed, then depressurization by operator action cannot be accomplished. Uncertainties include reliability of the PORVs, battery life, and air bottle depletion. The PORVs could stick closed due to component deformation or melting. Both the battery that operates the solenoid valve controlling air to the PORVs and the air bottles dedicated to the PORVs could become depleted during the accident. The battery life is estimated to be approximately 4 h with load shedding, and the air bottles have sufficient capacity for 80 cycles of the PORVs [23]. It appears that both are insufficient to carry out intentional depressurization. While the analyses indicate the theoretical feasibility of depressurization, additional battery life and air capacity may be required to actually accomplish depressurization in Surry.

## V. Summary and Conclusions

Based on these analyses, we conclude that there are four strategies to mitigate DCH. The first strategy is to attempt normal plant recovery by regaining ac power and/or auxiliary feedwater (AFW). If this cannot be done, then an emergency source of AFW such as use of the firewater system should be attempted. In both of these strategies, core damage can be prevented if the heat sink is restored. Timely restoration of the heat sink may require the operators to perform the above two tasks in parallel. This has the potential to add confusion and diffuse the recovery effort. If neither of the first two strategies are accomplished, then the PORVS should be opened to depressurize the RCS once the core has uncovered. This will depressurize the system to a low level near containment pressure. If the third strategy cannot be invoked, then a sequence with no operator action may still mitigate DCH. There is a chance that the surge line or possibly another primary system boundary will fail due to creep rupture or melting, and which would result in RCS depressurization.

The presence of ~~calculations~~, operational, and phenomenological uncertainties ~~that may affect these conclusions~~ has been identified. Studies of the potential negative effects such as hydrogen distribution in containment and molten fuel-coolant interactions are ongoing and required for closure of the intentional depressurization issue. Efforts are also continuing to reduce the uncertainties through systematic scrutiny of code models and comparative analyses. Further, the analyses presented in this paper are specific to the Surry Nuclear Power Plant. Conclusions may have to be modified for other plants.


## ACKNOWLEDGEMENT

Work supported by the U. S. Nuclear Regulatory Commission, Office of Nuclear Regulatory Research, under DOE Contract No. DE-AC07-76IDO1570.

## References


1. U. S. NRC, Severe Accident Risks: An Assessment for Five U.S. Nuclear Power Plants, NUREG-1150, Second Draft for Peer Review, April 17, 1989.

2. Loomis, G. G., and Cozzuol, J. M., Decay Heat Removal Using Feed-and-Bleed for U.S. Pressurized Water Reactors, NUREG/CR-5072, EGG-2526, June 1988.

3. Schultz, R. R., Fletcher, C. D., and Charlton, T. R., "Station Blackout in U.S. Light-Water Reactors, Nuclear Safety, Vol. 25, No. 4, July-August 1984.

4. Ransom V. H., et al., RELAP5/MOD1 Code Manual Volume 1: System Models and Numerical Models, NUREG/CR-1826, EGG-2070, November 1980.

5. Ransom V. H., et al., RELAP5/MOD2 Code Manual, NUREG/CR-4312, EGG-2396, August 1985.

6. Liles, D., et al., TRAC-PF1/MOD1, NUREG/CR-3858, LA-1057-MS, July 1986.

7. Ransom, V. H. and Trapp, J A., "Sound Speed Models for a Noncondensible Gas-Steam-Water Mixture," Proceedings of the Japan-U.S. Seminar on Two-Phase Flow Dynamics, Lake Placid, New York, July 29-August 3, 1984.

8. Driskell, W., E. and Hanson, R. G., "Summary of ICAP Assessment Results for RELAP5/MOD2," Transactions of the Sixteenth Water Reactor Safety Information Meeting, Gaithersburg, Maryland, October 24-27, 1988.

9. Broughton, J. M., Kuan, P., Petti, D. A., Tolman, E. L. , "A Scenario of the TMI-2 Accident," Nuclear Technology, to be published summer 1989.

10. Golden, D. W., et al., "Summary of the TMI-2 Analysis Exercise," Nuclear Technology, to be published summer 1989.

11. Allison, C. M., et al., SCDAP/RELAP5/MOD2 Code Manual, NUREG/CR-5273, to be published June 1989.

12. Camp, W., Tomkins, J., Heames, T., and Dearing, J., "Physical Modeling of the In-Vessel Phases of Severe Reactor Accidents - The Melprog/Trac Computer Code," International Symposium on Severe Accidents in Nuclear Power Plants, IAEA-SM-296/97, Sorrento, Italy, March 21-25, 1988.

13. Henrie, J. O., and Postma, A. K., Lessons Learned from Hydrogen Generation and Burning During the TMI-2 Event, GEND-061, May 1987.

14. Kuan, P. Assessment of TMI-2 Plenum Assembly Damage, EGG-TMI-8020, April 1988.

15. Chambers, R., Hanson, D. J., Dallman, R. J., Odar, F., "Depressurization To Mitigate Direct Containment Heating," Transactions of the Sixteenth Water Reactor Safety Information Meeting, Gaithersburg, Maryland, October 24-27, 1988.

16. Chung, H. M., Kassner, T. F., Embrittlement Criteria for Zircaloy Fuel Cladding Applicable to Accident Situations in Light Water Reactors., NUREG/CR-1344, ANL-79-48, January 1980.

17. Bayless, P. D., Analyses of Natural Circulation During a Surry Station Blackout Using SCDAP/RELAP5, NUREG/CR-5214, EGG-2547, October 1988.

18. Chambers, R., Galyean, W. J., Gilmore W. E., Accident Management of Surry Direct Containment Heating by Depressurization of the Reactor Coolant System - Progress Report, EGG-SSRE-7854, September 1987.

19. Kelly, J. E., "Advances in MELCOR Modeling and Analysis", Transactions of the Sixteenth Water Reactor Safety Information Meeting, NUREG/CP-0096, October 1988.

20. Heames, T. J. and Smith, R. C., "Integrated MELPROG/TRAC Analyses of a PWR Station Blackout," to be presented at the 1989 National Heat Transfer Conference, August 6-9, 1989, Philadelphia.

21. Virginia Power Company, Surry Power Station Updated Final Safety Analysis Report, Docket 05000280, July 16, 1982.

22. Swain, A. D., Accident Sequence Evaluation Program Human Reliability Procedure, NUREG/CR-4772, February 1987.

23. Bertucio, R. C. and Julius, J. A., Analysis of Core Damage Frequency: From Internal Events: Surry, Unit 1, NUREG/CR-4550, Revision 1, Volume 3, Draft for Comment, September 1988.

## NOTICE

that its use by such third party would not infringe privately owned rights. The views expressed in this report are not necessarily those of the U.S. Nuclear Regulatory Commission.

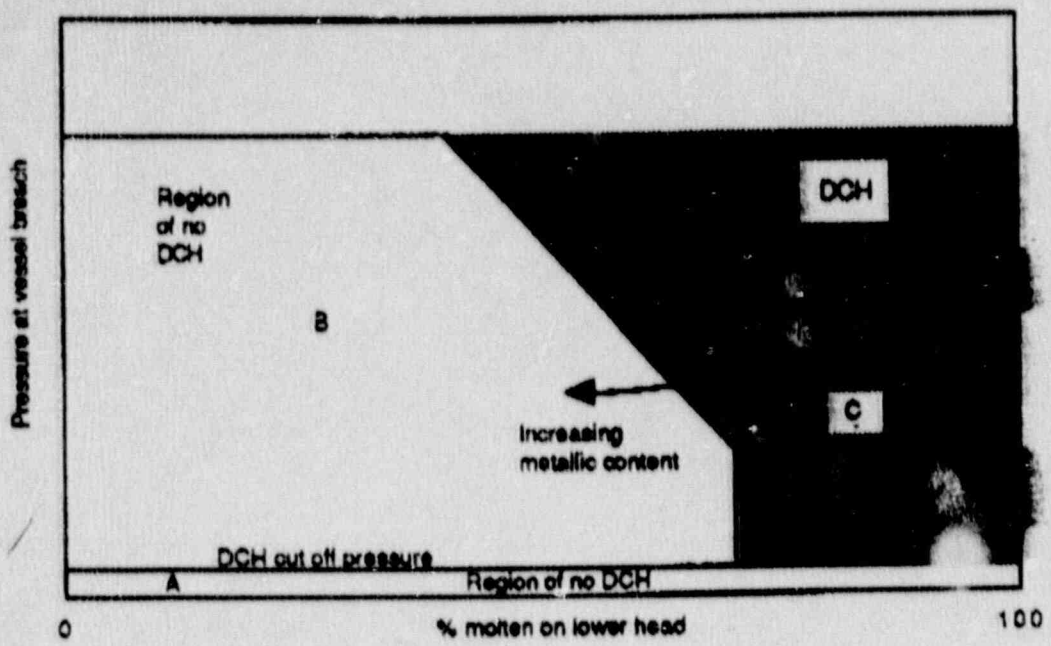


**Figure 1.** Conceptual direct containment heating map.

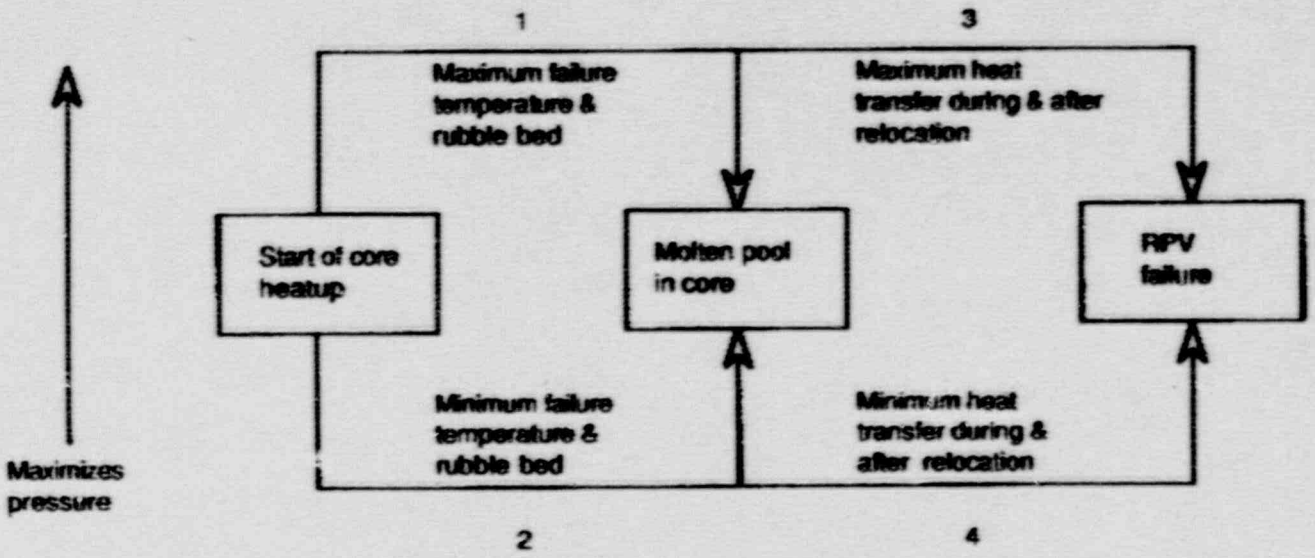


**Figure 2.** Calculation strategy to bound modeling uncertainties.

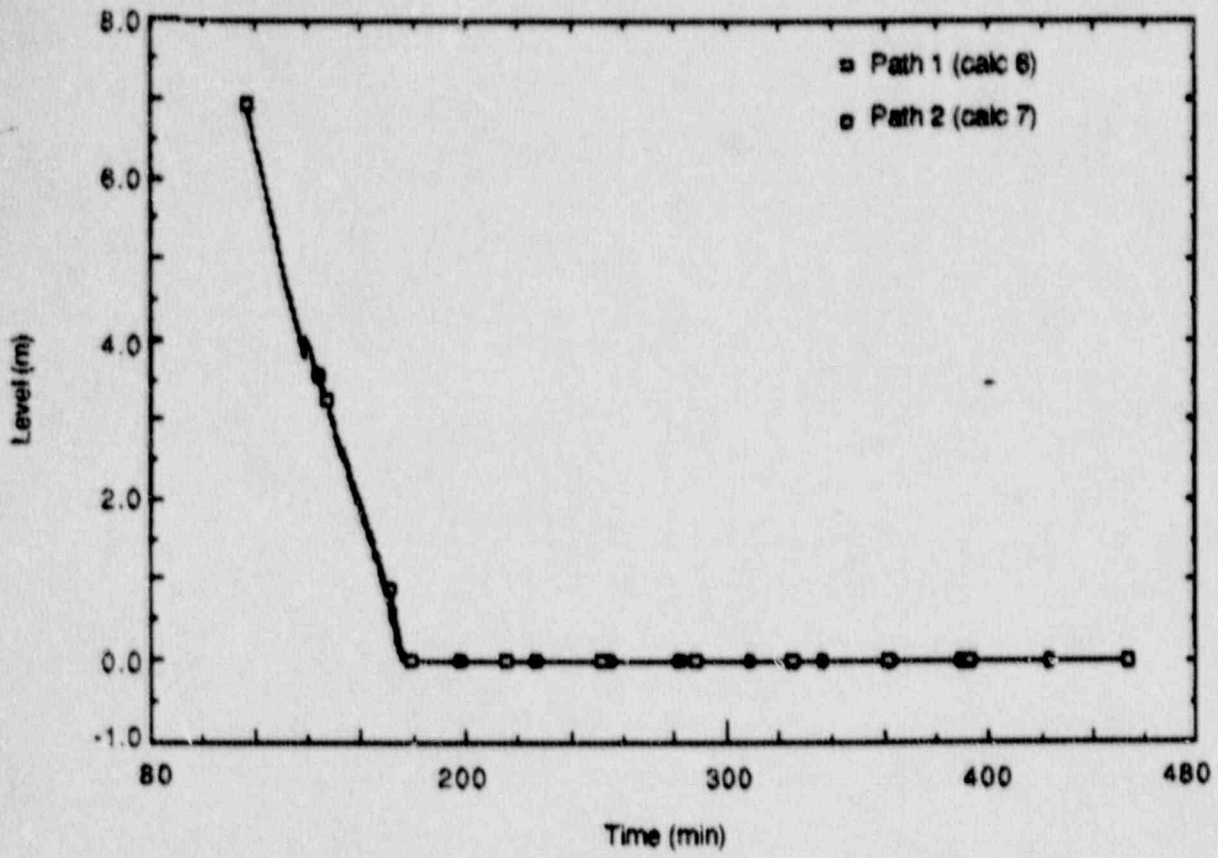


**Figure 3.** Calculated pressurizer level, early depressurization.

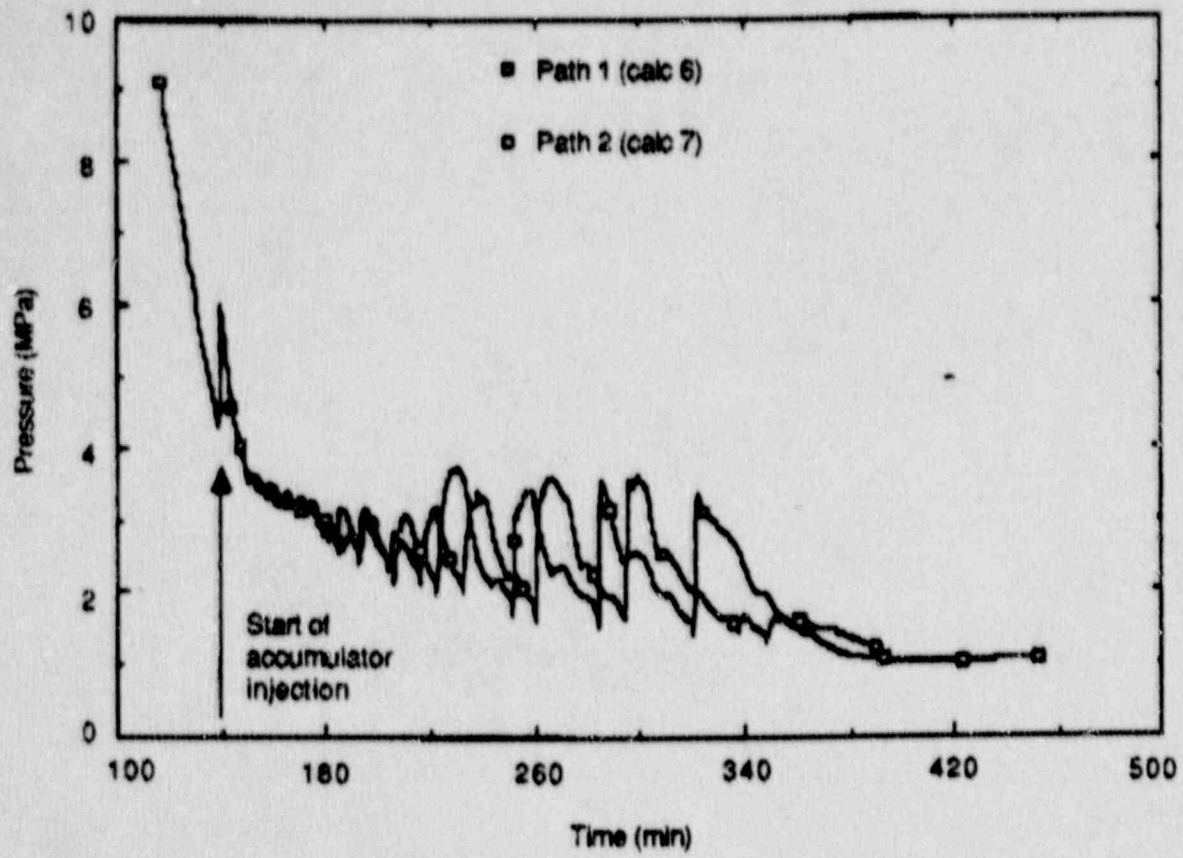


**Figure 4.** Comparison of calculated pressures, early depressurization.

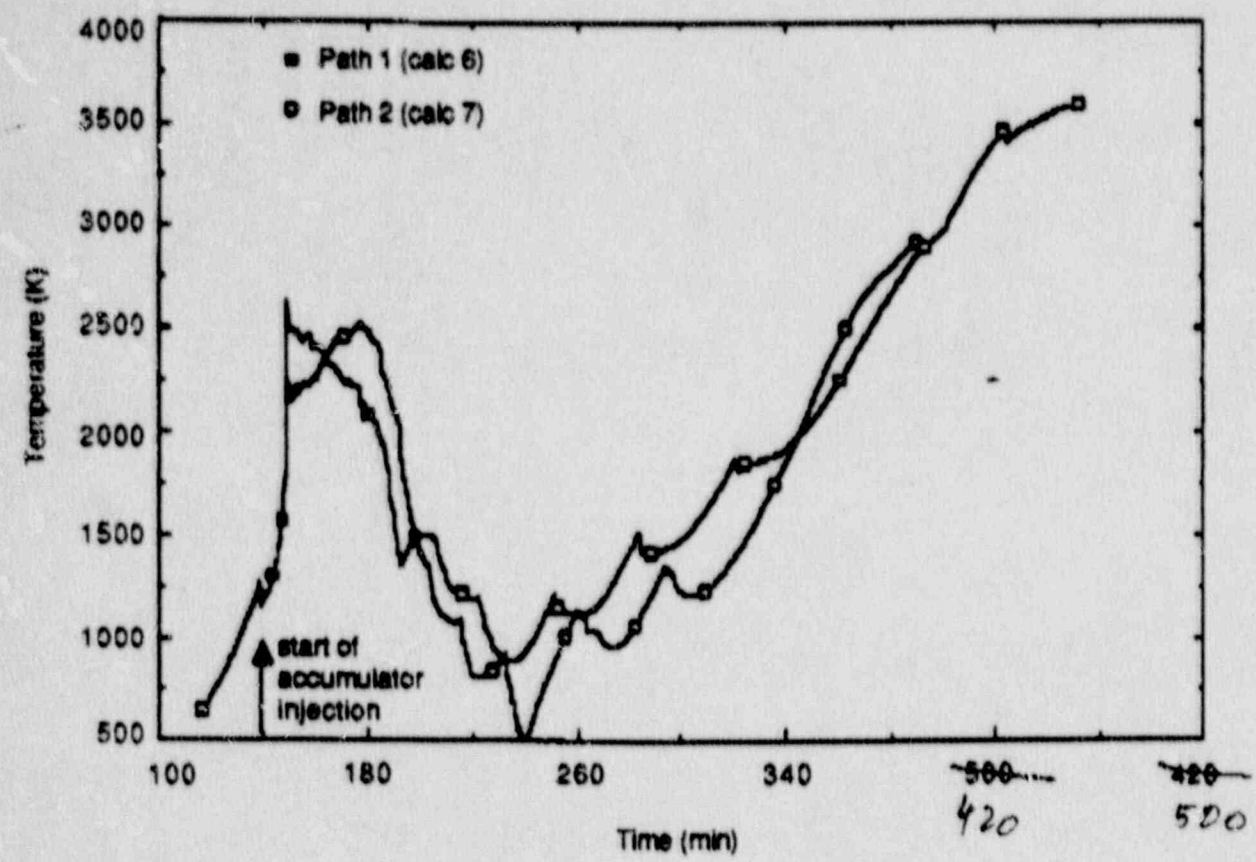


**Figure 5.** Comparison of calculated temperatures, early depressurization.

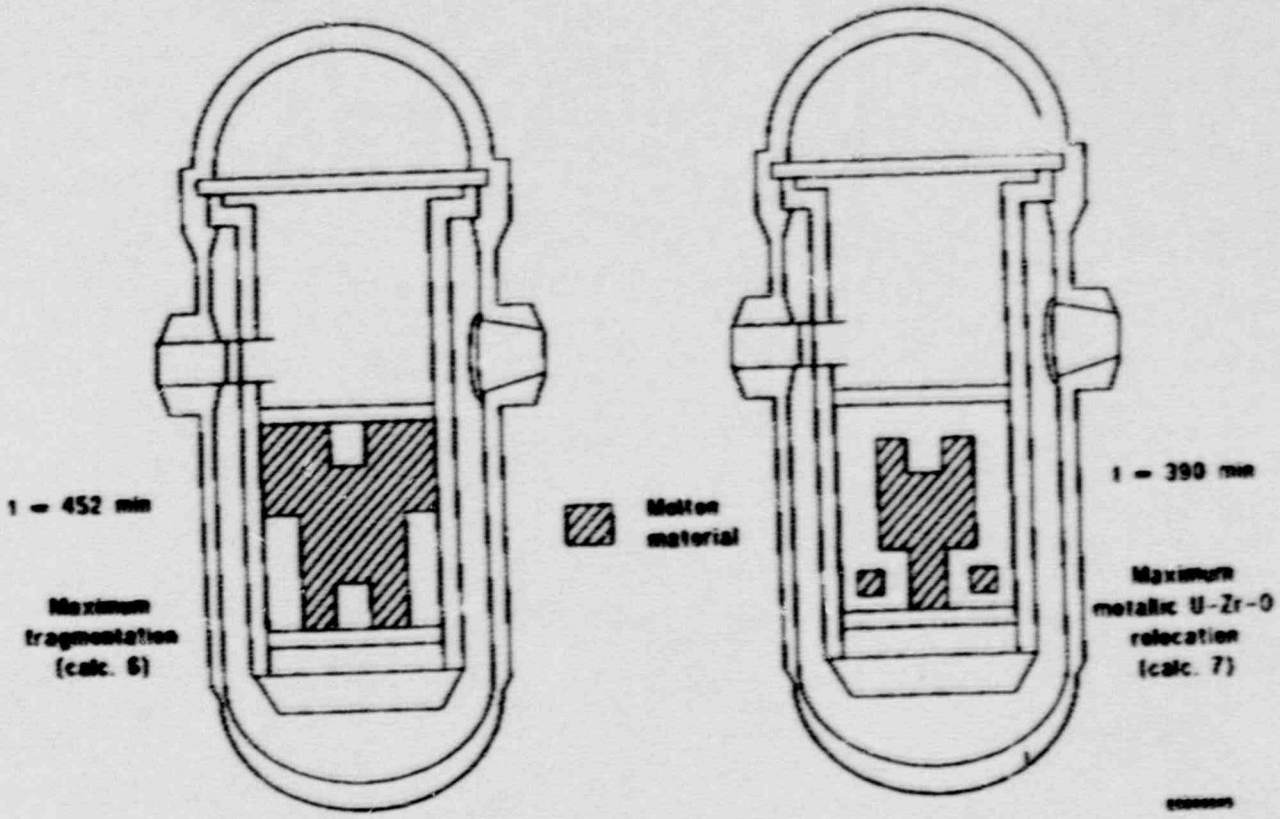


**Figure 6.** Comparison of calculated core geometries for paths 1 and 2, early depressurization.

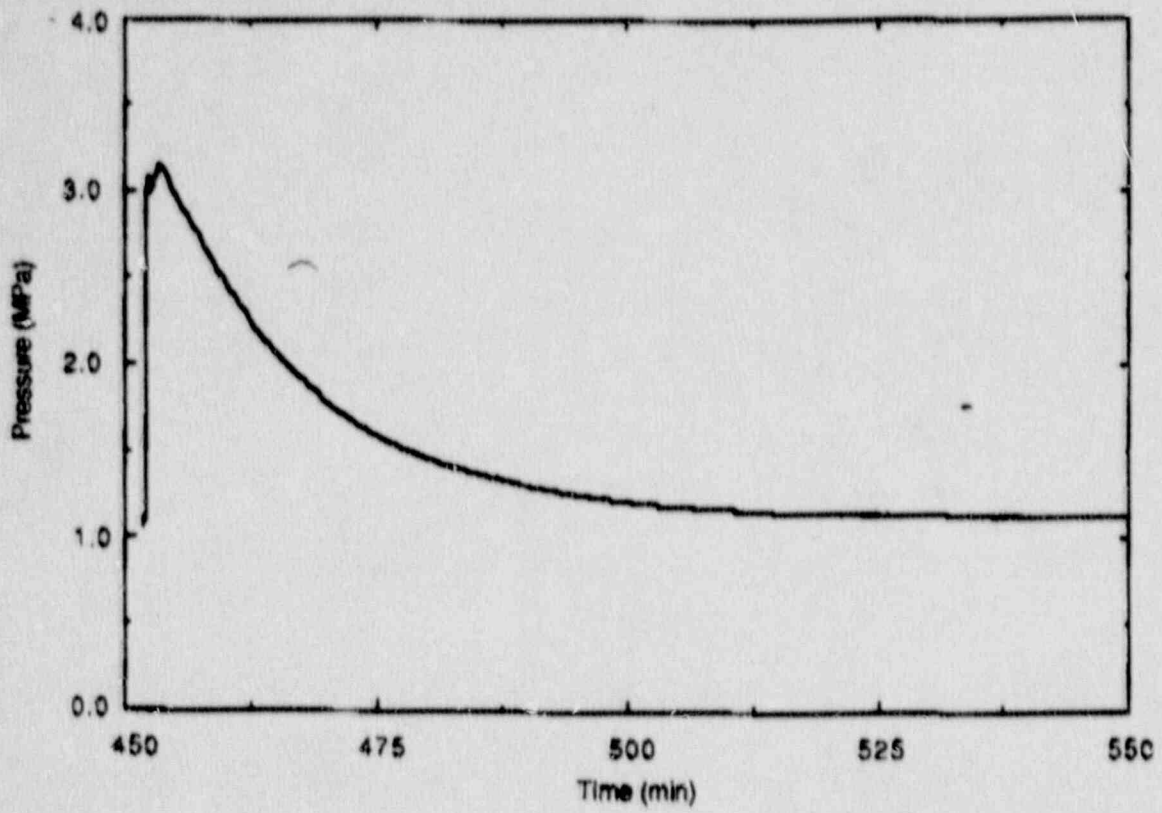


**Figure 7.** Calculated RCS pressure for path 3, early depressurization.

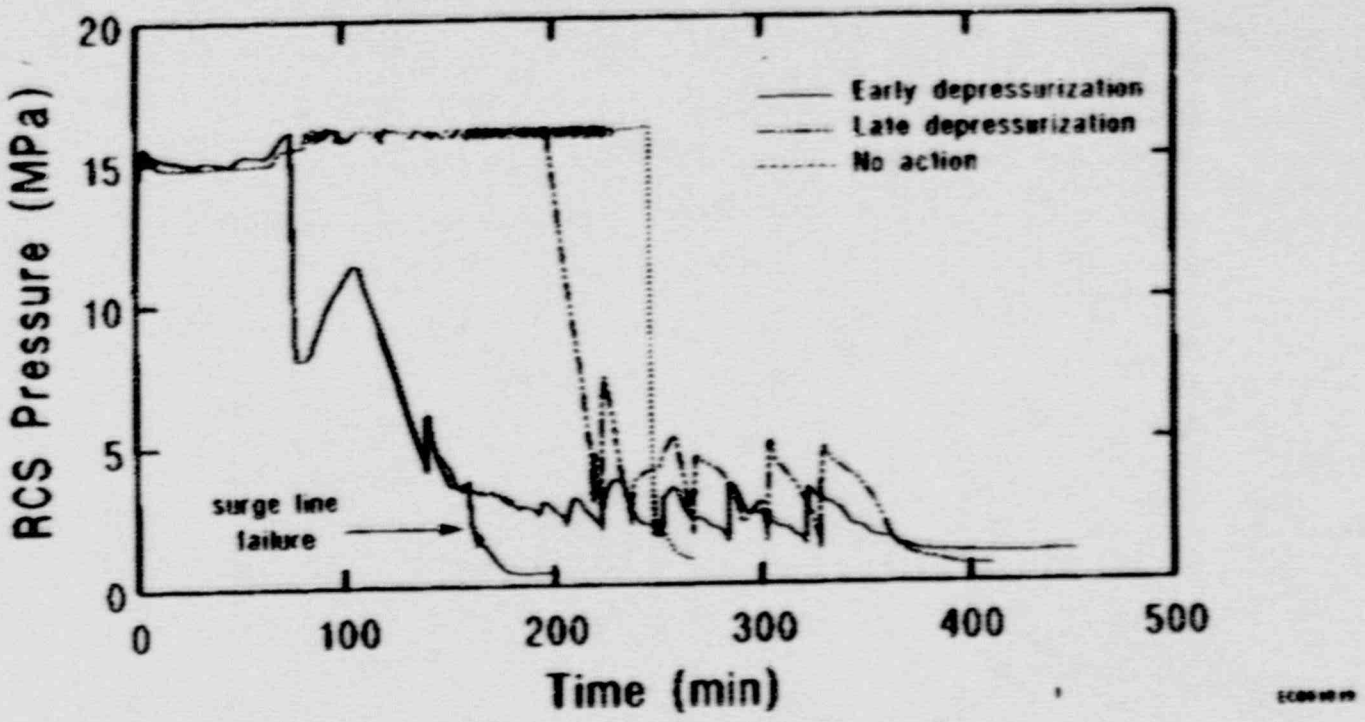


**Figure 8.** Comparison of calculated RCS pressures for early and late depressurization and no operator action strategies.

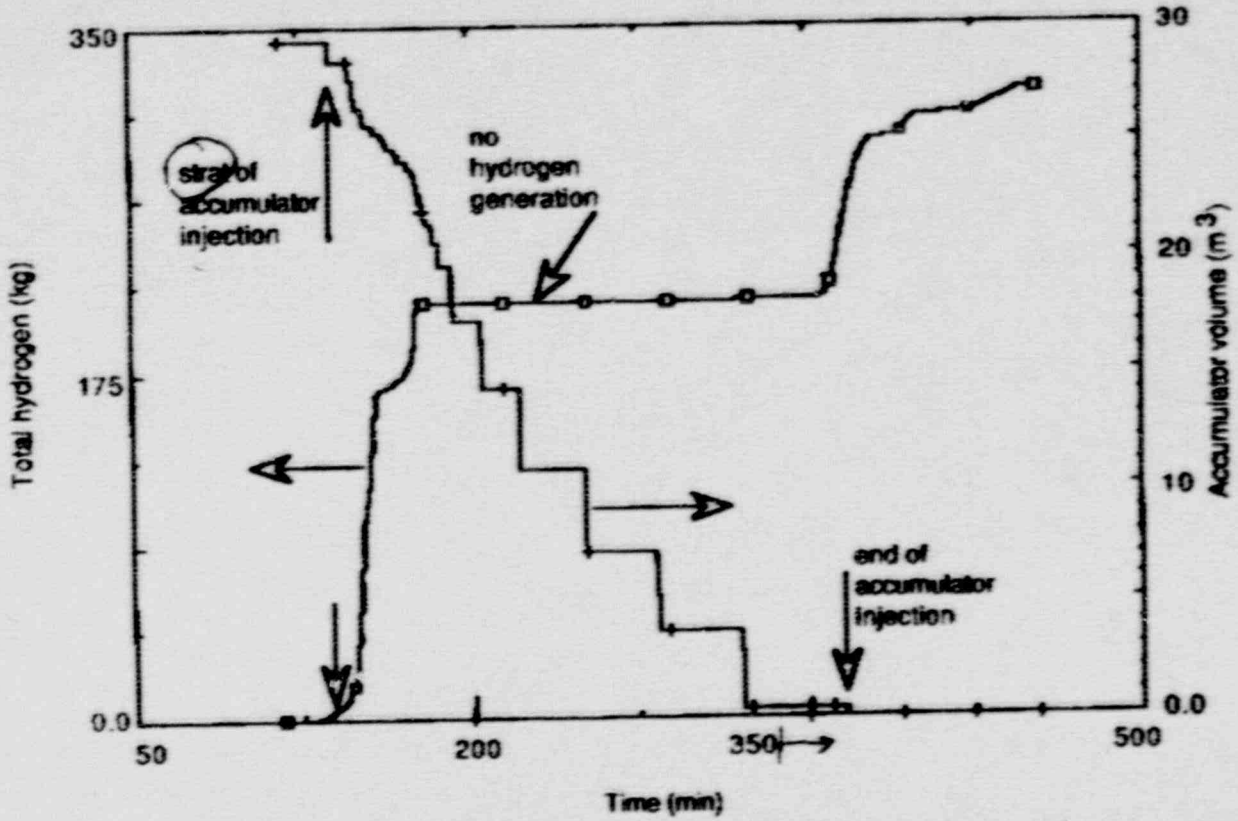


**Figure 9.** Total hydrogen generated compared to A loop accumulator volume, early depressurization.

Move 350 over
take out
unnecessary "ticks"

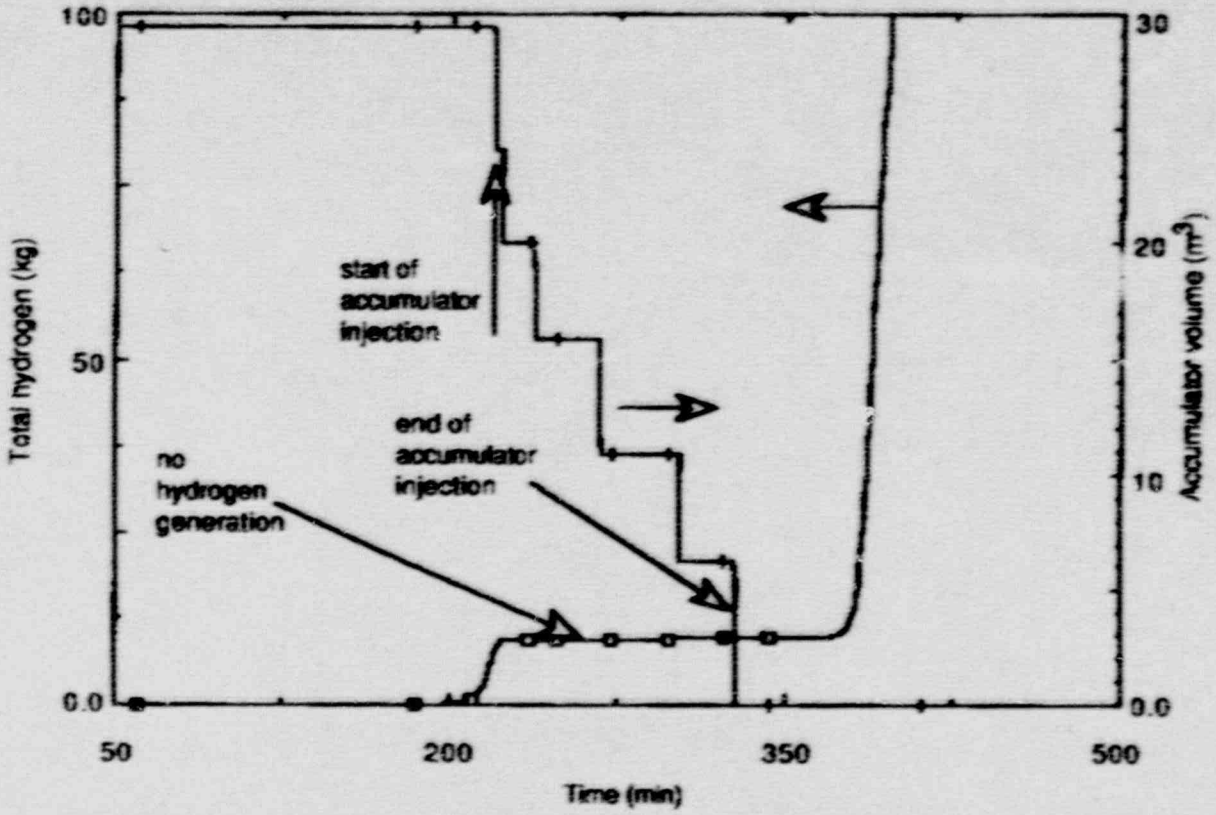


**Figure 10.** Total hydrogen generated compared to A loop accumulator volume, late depressurization.

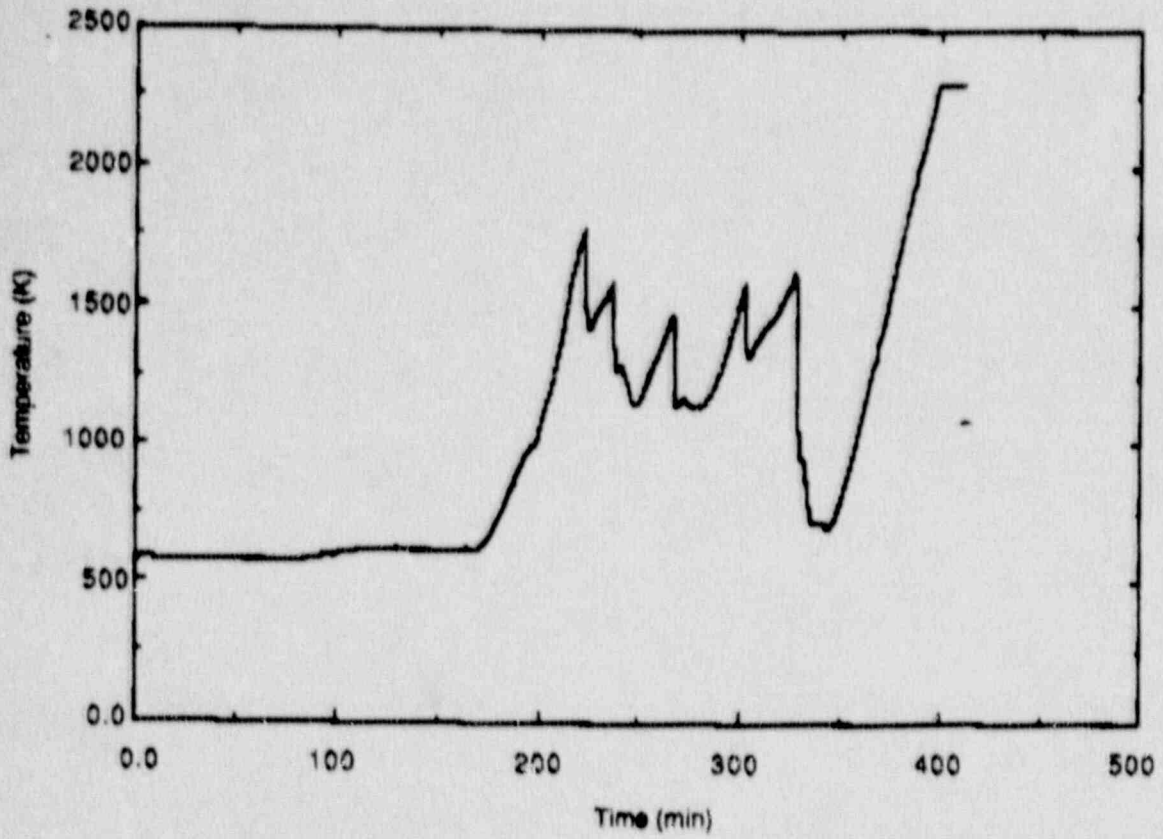


**Figure 11.** Calculated core temperature at top of core, late depressurization.

**Table I.** Calculation matrix used for the sensitivity studies.

| Calculations | Path (Fig 2) | Relocation Parameters | | Fragmentation Parameters | |
|---|---|---|---|---|---|
| | | $ZrO_2$ Temperature[a] | Percent Oxidized[b] | Cladding Temperature[c] | Beta Layer Thickness[d] |
| **Pressure boundary sensitivities** | | | | | |
| 1 - Intact surge line | e | 2500 K | 60 | e | |
| 2 - Failed surge line | e | 2500 K | 60 | e | |
| **Relocation sensitivities** | | | | | |
| 3 | 1 | 2680 K | 60 | Tsat+200K | 0.0001 m |
| 4 | 2 | 2300 K | 99.9 | Tsat+200K | 0.0001 m |
| 5 | 2 | 2400 K | 99.9 | Tsat+200K | 0.0001 m |
| **Core configuration sensitivities** | | | | | |
| 6 - Maximize rubble bed | 1 | 2680 K | 60 | 1273 K | 0.0001 m |
| 7 - Maximize fuel relocation | 2 | 2400 K | 99.9 | Tsat+90K | 0.0001 m |
| **Steam interaction sensitivities** | | | | | |
| 8 - Maximize steam interactions | 3 | | | | |
| 9 - Minimize steam interactions | 4 | | | | |

a Temperature at which $ZrO_2$ shell fails.

b Percent of Zr oxidation above which relocation will not take place.

c Temperature at which $ZrO_2$ will shatter in the presence of water.

d Thickness of the beta-Zr layer above which $ZrO_2$ will not shatter.

e Fragmentation not calculated. Calculations 1 and 2 present the system behavior when the fuel rods remain essentially intact and show the pressure and time sensitivity to failure of the pressure boundary.

Table II. Comparison of the results for paths 1 and 2.

| Event | Time (min) Calculation 6 (Path 1) | Calculation 7 (Path 2) |
|---|---|---|
| PORVs and head vent open | 75 | 75 |
| Start of cladding heatup | 114 | 114 |
| Start of accumulator injection | 139 | 139 |
| Calculated surge line failure | 166 | 172 |
| Fragmentation by quenching | 183 | 213 |
| In-core metallic U-Zr-O relocation | 366 | 149 |
| Accumulators empty | 367 | 348 |
| Molten pool formation | 400 | 378 |
| Molten material to lower plenum | 452 | 390 |

Table III. Comparison of the early, late, and no operator action strategies.

| Event | Time (min) Early (path 1) | Late (path 1) | No Operator Action |
|---|---|---|---|
| PORVs and head vent open | 75 | 192 | NA[1] |
| Start of cladding heat up | 114 | 171 | 160 |
| Start of accumulator injection | 139 | 218 | >245 |
| Calculated surge line failure | 166 | NC[2] | ~245 |
| Fragmentation by quenching | 183 | 215 | >245 |
| In-core metallic U-Zr-O relocation | 366 | 392 | ~245 |
| Accumulators empty | 367 | 328 | |
| Molten pool formation | 400 | tbc[3] | |
| Molten material to lower plenum | 452 | tbc | |
| RPV failure | ~600[4] | tbc | |

1. Not considered in calculation.
2. Not calculated to occur.
3. To be calculated.
4. Estimated based on heat up rate of lower head.